

See discussions, stats, and author profiles for this publication at: <https://www.researchgate.net/publication/228855426>

Colour Normalisation in Digital Histopathology Images

Article · January 2009

CITATIONS

45

READS

255

7 authors, including:



Derek Magee

University of Leeds

135 PUBLICATIONS 1,221 CITATIONS

[SEE PROFILE](#)



Michael Shires

University of Leeds

48 PUBLICATIONS 770 CITATIONS

[SEE PROFILE](#)



Kevin Mohee

Hull and East Yorkshire Hospitals NHS Trust

21 PUBLICATIONS 66 CITATIONS

[SEE PROFILE](#)



Philip Quirke

University of Leeds

634 PUBLICATIONS 29,849 CITATIONS

[SEE PROFILE](#)

Some of the authors of this publication are also working on these related projects:



Pathological Society Strategy [View project](#)



<http://www.medicalimagemanager.com> [View project](#)

All content following this page was uploaded by [Derek Magee](#) on 26 December 2013.

The user has requested enhancement of the downloaded file.

Colour Normalisation in Digital Histopathology Images

Derek Magee¹, Darren Treanor², Doreen Crellin², Mike Shires², Katherine Smith², Kevin Mohee², and Philip Quirke²

¹ School of Computing, University of Leeds, Leeds, UK, D.R.Magee@leeds.ac.uk,

² Pathology and Tumour Biology, Leeds Institute of Molecular Medicine, University of Leeds, Leeds, UK,

Abstract. Colour consistency in light microscopy based histology is an increasingly important problem with the advent of Gigapixel digital slide scanners and automatic image analysis. This paper presents an evaluation of two novel colour normalisation approaches against the previously utilised method of linear normalisation in $l\alpha\beta$ colourspace. These approaches map the colour distribution of an over/under stained image to that of a well stained target image. The first novel approach presented is a multi-modal extension to linear normalisation in $l\alpha\beta$ colourspace using an automatic image segmentation method and defining separate transforms for each class. The second approach normalises in a representation space obtained using stain specific colour deconvolution. Additionally, we present a method for estimation of the required colour deconvolution vectors directly from the image data. Our evaluation demonstrates the inherent variability in the original data, the known theoretical problems with linear normalisation in $l\alpha\beta$ colourspace, and that a multi-modal colour deconvolution based approach overcomes these problems. The segmentation based approach, while producing good results on the majority of images, is less successful than the colour deconvolution method for a significant minority of images as robust segmentation is required to avoid introducing artifacts.

1 Introduction

Histopathology involves the diagnosis of disease by examination of tissue samples prepared using coloured chemical stains that bind selectively to proteins. Colour constancy is a problem in histology based on light microscopy due to; variable chemical colouring/reactivity from different manufacturers/batches, colouring being dependent on staining procedure (timing, concentrations etc.), and light transmission being a function of section thickness. [1] outlines the need for standardisation of reagents and procedures in histological practice. However, such rigorous standardisation is not practised in the majority of laboratories and complete standardisation is not possible without purer (and less variable) reagents (requiring input from chemical manufacturers, and associated increase in cost).

With the advent of digital imaging and automatic image analysis this has become more of an issue. For example, many commercial automatic image analysis algorithms (e.g. the cell nucleus counting algorithm from Aperio www.aperio.com)

require parameters defining the expected colour distribution of anatomy of interest and fail if these parameters are incorrect. Conventional colour constancy ideas (see [2] for a good overview) are inappropriate as they are typically based on a Lambertian (reflective) model of image formation, whereas light microscopy images are formed via light transmission through the sample. Consequently, the majority of works in the area of automatic image analysis of colour histology images bypass the problem of colour constancy by transforming the images to greyscale (for example [3, 4]). This is successful in cases where greyscale intensity is the primary cue (e.g. many types of cell nuclei are much darker under certain stains than surrounding anatomy). However, this ignores the wealth of information in the colour representation used routinely by histologists. Typically, multiple (2 or 3) different coloured stains are used to indicate the presence of different proteins. The intensity of each colour is related to the concentration of the corresponding protein. Additionally, more than one protein may be present in a given area (resulting in a mix of colours). Converting images to greyscale results in an image representing total concentration of all proteins.

One work that has explicitly utilised colour (rather than converting to greyscale) is the recent work of Wang *et al.* [5] in which a colour normalisation method is applied prior to colour based analysis. The method of Reinhard *et al.* [6] is used, in which a set of images are mapped to the colour distribution of a target image on a per-pixel basis by equalising the mean and standard deviations separately for each dimension of a perceptual ($l\alpha\beta$) colourspace. The drawback is that this ignores the inherent multimodality of this data. There is no reason why foreground and background and areas stained by different stains should be normalised by the same transform, as many of the causes of variation are a function of the chemical stain and process used (each stain being applied separately in sequence). The approach works for the images in [5] as single stain (Eosin) dominates in terms of area, and their second stain (Haematoxylin) is sufficiently low in intensity for such images (in comparison to Eosin) that poor normalisation of these pixels does not detract from classification performance. However, this does not hold in the general case. Later we show that linear normalisation in $l\alpha\beta$ colourspace can result in background areas being mapped as coloured regions, and foreground being incorrectly mapped. In the original paper [6] the problem of multimodality was highlighted and a solution suggested based on manual segmentation and separate application of the method to different areas.

In this paper a number of novel colour normalisation algorithms for digital histology images based on mapping images to a target are evaluated against linear normalisation in $l\alpha\beta$ colourspace. The first novel method is based on the linear normalisation in $l\alpha\beta$ colourspace method, extended to multiple pixel classes using a probabilistic (Gaussian Mixture Model based) colour segmentation method. Linear normalisation is applied separately for each pixel class (where class membership is defined by a pixel being coloured by a particular chemical stain, or being uncoloured i.e. background). This approach assumes an additive colour model (which is a reasonably poor model of the physics of light microscopy image formation [7]).

The second novel method presented is based on normalisation in a stain-specific colour deconvolution representation [7]. In this representation each di-

mension represents the amount by which a pixel is stained by a particular chemical stain. In one variant a linear normalisation is applied in this representation. In a second variant separate transforms are defined for foreground and background.

2 Methods and Materials

2.1 Data Preparation and Collection

Two data sets were acquired from our existing digital slide repository. Tissue was formalin fixed, paraffin embedded, and cut in ≈ 5 micron sections. The first set (“H&E”) was 48 slides of cirrhotic liver from 4 sub-sets (12 images/sub-sets) stained with Mayers Haematoxylin and Eosin counterstain. Each sub-set was prepared by the same technician using the same protocol. However, technician and chemical stain batch varied between sub-sets. The second set (“DAB”) was 12 images of colorectal carcinoma stained with antibodies against CD34 (Dako Envision detection system www.dako.co.uk). These were all prepared by the same technician using the same protocol. Virtual slides were obtained by scanning glass slides at 100,000 dpi using an Aperio XT scanner (Aperio, San Diego). Representative 1000×1000 sections at native zoom were extracted from these gigapixel images via the ImageServer http interface (JPEG quality=100%).

2.2 “Reinhard’s Method”

Reinhard *et al.* present a method [6] for matching the colour distribution of an image to that of a target image by use of a linear transform in a perceptual colour space (the $l\alpha\beta$ colour space of Ruderman *et al.* [8]) so as to match the means and standard deviations of each colour channel in the two images in that colour space. It has recently been applied to digital histology images stained with the Haemotoxin and Eosin (H&E) stains by Wang *et al.* [5] (among others) using a single linear transform for all pixels (i.e. not per class as suggested in [6]). Equations 1-3 describe this process, and are applied at each pixel.

$$l_{mapped} = \frac{l_{original} - \bar{l}_{original}}{\hat{l}_{original}} \hat{l}_{target} + \bar{l}_{target} \quad (1)$$

$$\alpha_{mapped} = \frac{\alpha_{original} - \bar{\alpha}_{original}}{\hat{\alpha}_{original}} \hat{\alpha}_{target} + \bar{\alpha}_{target} \quad (2)$$

$$\beta_{mapped} = \frac{\beta_{original} - \bar{\beta}_{original}}{\hat{\beta}_{original}} \hat{\beta}_{target} + \bar{\beta}_{target} \quad (3)$$

Where $\bar{l}, \bar{\alpha}$, and $\bar{\beta}$ are the channel means and $\hat{l}, \hat{\alpha}$, and $\hat{\beta}$ are the channel standard deviations (calculated over all pixels in the image).

2.3 An Automatic Segmentation Extension to Reinhard’s Method

Reinhard *et al.* [6] suggest manually segmenting different pixel classes (e.g. sky, trees, etc.) in both the image to be modified and the target image, and applying linear normalisation in $l\alpha\beta$ colourspace separately for each pixel class (although results of this are not presented in [6]). However, it is not feasible to manually segment large (typically $\approx 100K \times 80K$ pixel) digital histology images into areas of different staining purely for the purposes of colour normalisation. Additionally, it is likely that some pixels are stained with multiple stains (so cannot be assigned to a single class). However, automatic colour based segmentation is a well studied area within image analysis. The problem with this is (by definition) we do not have colour constancy. This makes segmentation a harder problem. Our solution is per-pixel colour segmentation using a probabilistic prior and a Variational-Bayesian Gaussian Mixture model (see [9], Chapter 10). Priors are estimated for the colour of pixels belonging to each of the 2 stains used in a particular image, plus pixels belonging to the background, and this information is incorporated into the estimation of the mixture model using a variational (EM-like) estimation process (figure 1) [9]. Our method of calculating these priors is to hand segment areas of a small selection of images of a particular stain and calculate the mean colour of each pixel class (P_{mean_k}). Other elements of the prior (P_{cov_k} , α_0, β_0 and v_k) are set to sensible values defined by hand by cross validation against a small training set of images (separate from the set used in the evaluation later). Ad-hoc tests suggest this approach works for many examples where a mixture model estimated using the EM algorithm or K-means clustering fails.

Initialisation	step 1	step 2
Mixture Precision	$\ln p_{nk} = \mathbb{E}_{\pi_k} - 0.5\mathbb{E}_{\Lambda_k} - 0.5\mathbb{E}_{\mu_k}$	$\alpha_k = \alpha_0 + N_k$
Matrices	$\mathbb{E}_{\pi_k} = \psi(\alpha_k) + \psi(\sum_k \alpha_k)$	$\beta_k = \beta_0 + N_k$
$W_0^{-1} = P_{cov_k} N_p$	$\mathbb{E}_{\Lambda_k} =$	$m_k = \frac{1}{\beta_k}(\beta_0 m_0 + N_k \bar{x}_k)$
$W_k^{-1} = W_0^{-1}$	$\sum_{i=1}^D \psi(\frac{v_k+1-i}{2}) + D \ln 2 + \ln W_k $	$W_k^{-1} = W_0^{-1} + N_k S_k +$
Mixture Means	$\mathbb{E}_{\mu_k} = D\beta_k^{-1} +$	$\frac{\beta_0 N_k}{\beta_0 + N_k}(\bar{x}_k - m_0)(\bar{x}_k - m_0)^T$
$m_k = m_{0_k} = P_{mean_k}$	$v_k(x_n - m_k)^T W_k(x_n - m_k)$	$v_k = v_0 + N_k + 1$
Other parameters	$r_{nk} = p_{nk} / \sum_{j=1}^3 p_{nj}$	
$\alpha_k = \alpha_{0_k} = 0.5N_p$	$N_k = \sum_{n=1}^{N_p} r_{nk}$	
$\beta_k = \beta_{0_k} = 0.5N_p$	$\bar{x}_k = \frac{1}{N_p} \sum_{n=1}^{N_p} r_{nk} x_n$	
$v_k = v_{0_k} = 0.75N_p$	$S_k =$	
	$\frac{1}{N_p} \sum_{n=1}^{N_p} r_{nk} (x_n - \bar{x}_k)(x_n - \bar{x}_k)^T$	

Fig. 1. Estimation of a 3 colour Gaussian Mixture Model (2 stains plus background, one mixture per colour) in an image using a Variational Bayesian approach. Steps 1 & 2 (taken directly from [9]), are repeated until convergence. For a derivation of steps 1 & 2 see [9], chapter 10.2. N_p is the number of pixels used.

Reinhard’s method is applied by either assigning each pixel to the class with the largest probability (r_{nk} , from figure 1) and applying Reinhard’s method separately for each class (suggested in [6]); “VB-Reinhard-Hard”, or weighting the colour mean estimation, standard deviation estimation, and transform calculation by r_{nk} (equations 4, 5 and 6 respectively); “VB-Reinhard-Weighted”.

$$\bar{X}_{l\alpha\beta_k} = \frac{1}{N_k} \sum_{n=1}^{N_p} r_{nk} X_{l\alpha\beta_n} \quad (4)$$

$$\sigma_{l\alpha\beta_k} = \frac{1}{N_k} \sum_{n=1}^{N_p} r_{nk} (X_{l\alpha\beta_n} - \bar{X}_{l\alpha\beta_k})^2 \quad (5)$$

$$\hat{X}_{l\alpha\beta_n} = \sum_{k=1}^3 r_{nk} (X_{l\alpha\beta_n} - \bar{X}_{l\alpha\beta_k}(\text{image})) \sigma_{l\alpha\beta_k}(\text{target}) / \sigma_{l\alpha\beta_k}(\text{image}) + \bar{X}_{l\alpha\beta_k}(\text{target}) \quad (6)$$

Where $X_{l\alpha\beta_n}$ is the colour of pixel n in $l\alpha\beta$ colourspace, $\bar{X}_{l\alpha\beta_k}$ is the mean $l\alpha\beta$ value of component k (background, stain 1, or stain 2), $\sigma_{l\alpha\beta_k}$ is the standard deviations of the $l\alpha\beta$ channels of component k , and $\hat{X}_{l\alpha\beta_n}$ is the normalised $l\alpha\beta$ colourspace values of pixel n . N.B. $\bar{X}_{l\alpha\beta_k}$ and $\sigma_{l\alpha\beta_k}$ are calculated for both the target image and the image to be normalised (as required by equation 6).

2.4 A Colour Deconvolution Based Method for Colour Normalisation

The method described in the previous section assumes an additive colour model i.e. a pixel is a weighted sum of 3 colours (2 stains plus background). Ruifrok [7] presents a physics based argument (based on Lambert- Beers law) for the colour formation process in microscopy being a subtractive process (equation 7).

$$I = I_0 \exp(-Ac) \quad (7)$$

Where I_0 is the intensity of light entering the specimen (RGB colourspace), I is the light detected (RGB colourspace), A is the amount of stain(s) and c is a matrix related the absorption factor(s) of the stain(s) (see [7] for details). The $\exp()$ operator is a vector operator in this case, applying the exponential function to each RGB channel separately. A may be estimated, and used as a new representation ($A = [a_1, a_2, a_3]$), for up to 3 stains (or 2 stains and a ‘complement’) from a single observation I if c is known for the set of stains.

We have implemented two novel colour mapping/normalisation approaches based on colour deconvolution and target image matching in deconvolution space. Normalised RGB values can be recovered using equation 7. We use our own implementation of [7] working with floating point representations and applying an upper limit to the channel values of 500 rather than 255, unlike other implementations (see www.dentistry.bham.ac.uk/landinig/software/cdeconv/cdeconv.html) that work with 8 bit integer data. This is important for fidelity when recombining colour channels to generate an RGB image. Deconvolving and re-combining using an 8 bit integer representation (with no normalisation) results in a significantly changed image. However, with our implementation images may be reconstructed with high accuracy.

The first approach (“CDV-L”) uses a linear transform to match means and standard deviations in each dimension of this representation (as in section 2.2). The disadvantage with the linear approach is that the same transform is applied to both foreground and background pixels, which can effect the distinction

between these (i.e. background can take on the colour of the stain). We implemented a multi-modal version of this method (“CDV-MM”). This uses a two component 1D Gaussian mixture model (estimated using a Variational Bayesian approach - see previous section) in each dimension to separate foreground from background. To increase the appropriateness of this mixture of two Gaussian model near chemically saturated pixels (any channel value <25) and any completely white pixels (channel value >300) are excluded from this estimation process (these would otherwise bias the means downwards, and upwards respectively away from the peaks of the distributions). The output value is a weighted combination of linear corrections based on foreground mean and standard deviation matching (\hat{A}_{fg}), background mean and standard deviation matching (\hat{A}_{bg}) and the original value (A), as in equation 8. The original value is used to ensure large values (near-pure white pixels) are not modified.

$$\hat{A} = \frac{1}{w_{fg} + w_{bg} + w_{id}} \left(w_{fg} \hat{A}_{fg} + w_{bg} \hat{A}_{bg} + w_{id} A \right) \quad (8)$$

Weights are calculated by a combination of linear and Gaussian interpolation. The reason is most pixels clearly belong to either foreground or the background. Thus, interpolation based on Gaussian probabilities is sensible (linear interpolation gives undue influence to the ‘wrong’ transform). However, the Gaussian approach introduces artifacts near pixels that lie on the class boundary (transition can be abrupt). Combining Gaussian and linear interpolation gives a function that exhibits both no class-transition artifacts and approximates well to \hat{A}_{fg} , \hat{A}_{bg} or A for pixels that clearly belong to the corresponding class (equation 9).

$$[w_{fg}, w_{bg}, w_{id}] = \begin{cases} [1, 0, 0] & \text{if } A < \bar{A}_{fg} \\ [G_{av} G_{fg} + (1 - G_{av}) D_{bg}, & \text{if } A > \bar{A}_{fg} \text{ and } A < \bar{A}_{bg} \\ G_{av} G_{bg} + (1 - G_{av}) D_{fg}, 0] & \\ [0, 1 - P_{white}, P_{white}] & \text{if } A > \bar{A}_{bg} \end{cases} \quad (9)$$

Where G_{fg} and G_{bg} are [0:1] normalised Gaussian functions using foreground and background mixture parameters respectively, $G_{av} = G_{fg} + G_{bg}$, and D_{fg} and D_{bg} is the [0:1] normalised distance between A and the mean of the foreground and background mixtures respectively. P_{white} is the probability the pixel is white (a [0:1] normalised Gaussian in RGB space with mean [255,255,255] and equal diagonal covariance of 25). Relative contributions are weighted by G_{tot} so the interpolation is Gaussian (roughly nearest neighbour) if the $P(pixel|mixture)$ is high (for either mixture), reverting to linear interpolation otherwise.

Estimation of Image Specific Colour Deconvolution Vectors Estimation of colour deconvolution vectors (c) for each stain from (the mean of) a small number of manually selected pixels in samples stained with a single stain is the approach suggested in [7]. This has the disadvantage that such a sample set must be prepared for each batch at the same time as the images using the same protocol (precluding retrospective analysis). Even if this is possible, we have observed significant variation within a single batch of images in our data

(see later). One solution is to use standard vectors for particular stains provided with freely available implementations of [7]. However, we have found estimating vectors on a per-image basis (based on manually selected areas from the images themselves) produces visually better stain separation than using these standard values. Annotation of (approximately 500) pixels for each of the two stains takes around 2 minutes per image using our in-house tool. An alternative is to use the output of the segmentation method described in section 2.3. Selecting pixels where $r_{nk} > T_r$ for a particular stain (where T_r used is 0.95) produces usable vectors in the majority of cases. Instances where this doesn't work well relate to images where the colour distributions of the channels overlap significantly (i.e. poor quality staining) and thus the presented segmentation approach fails badly. However, Reasonable quality vectors may be estimated by this process even if a segmentation based on r_{nk} is of visually imperfect quality.

2.5 Evaluation Methodology

The image data sets described in section 2.1 were processed (using a single target image per data set) using the 5 different colour normalisation algorithms described previously; Reinhard's method (section 2.2), the two segmentation-based variants of Reinhard's method (section 2.3), and the two methods based on colour deconvolution (section 2.4). For the H&E set colour deconvolution vectors were estimated automatically using the approach described in the previous section, with 5/48 vectors replaced by vectors based on a manual segmentation (on the basis of inspection of the deconvolved images). For the (smaller) H-DAB data set the vectors were all estimated based on manual segmentation.

Areas corresponding to Haematoxylin, either Eosin or DAB (depending on the data set) and background were identified using an interactive segmentation tool developed in our lab. Around 1000-2000 pixels were identified for each pixel type per image. The mean and covariance matrix of each region in the RGB representation was calculated and the Hotelling's T-square statistic (T^2 - a multivariate version of the T-test) calculated against the target distribution.

3 Results

Boxplots of T^2 values for each method are shown in figures 2 and 3. To give context; a pair of distributions calculated from sample size of 1000 with equal diagonal covariance displaced by 1 standard deviation in each direction results in a T^2 value of 1500. Values around, or below, this would indicate good agreement. Example normalised images are presented in figures 4 and 5.

4 Discussion

For the H&E set noticeable modes of failure were; i) Complete failure (e.g. figure 4 row6, column 2); VB-Reinhard-H (16 images), CDV-L (4 images), ii) Overstained/saturated nuclei; VB-Reinhard-H (20 images), and iii) significant staining of the background; Reinhard (6 images), CDV-L (2 images). In the quantitative evaluation the CDV-MM method shows the best consistency between normalised images and the target over all area types (improved from the

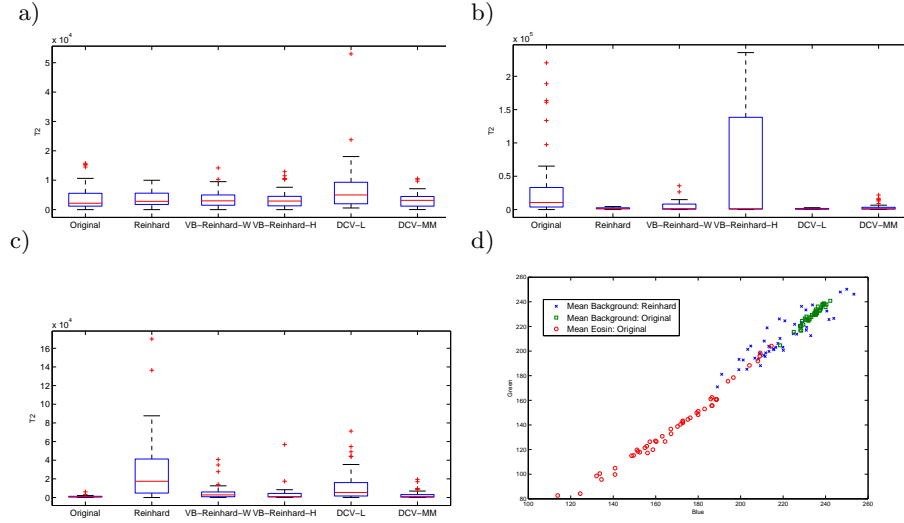


Fig. 2. H&E-Dataset: Consistency of RGB Colouring in manually selected areas of Haematoxylin staining, Eosin staining and background w.r.t. the target image for original images and images normalised using different colour normalisation methods; a) Haematoxylin, b) Eosin, c) Background. d) Scatterplot of mean background colour for original and Reinhard-corrected images with Mean Eosin colour.

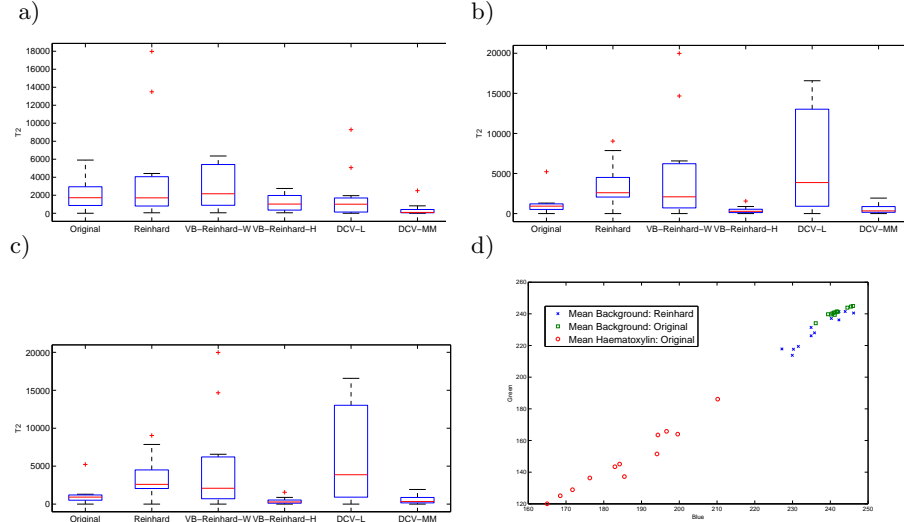


Fig. 3. DAB-Dataset: Consistency of RGB Colouring in manually selected areas w.r.t. the target image for original images and images normalised using different colour normalisation methods; a) Haematoxylin, b) DAB, c) Background. d) Scatterplot of mean background colour for original and Reinhard-corrected images with Mean Haematoxylin colour.

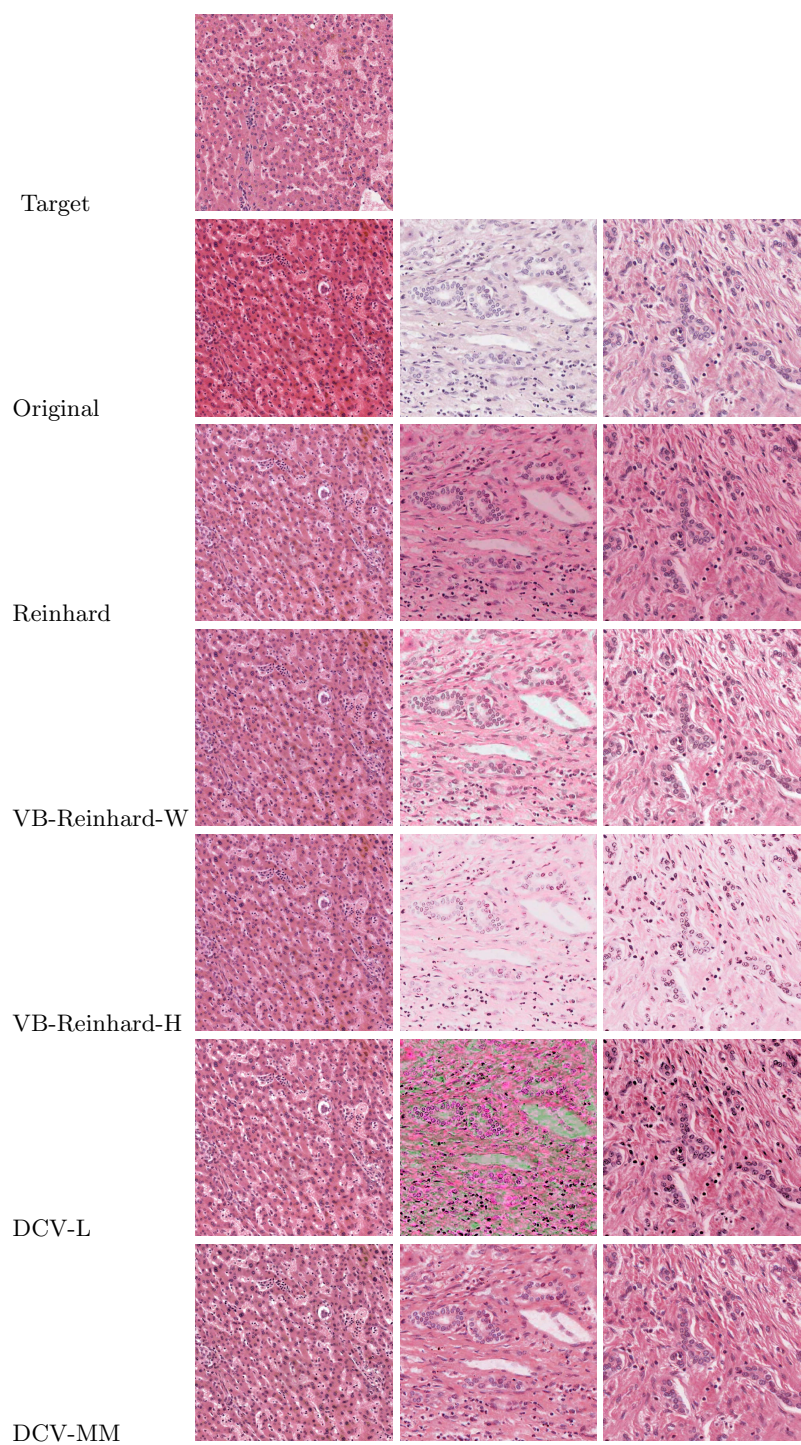


Fig. 4. Results of the different methods applied to 3 images of Haematoxylin and Eosin stained liver tissue. The first row contains the target image.

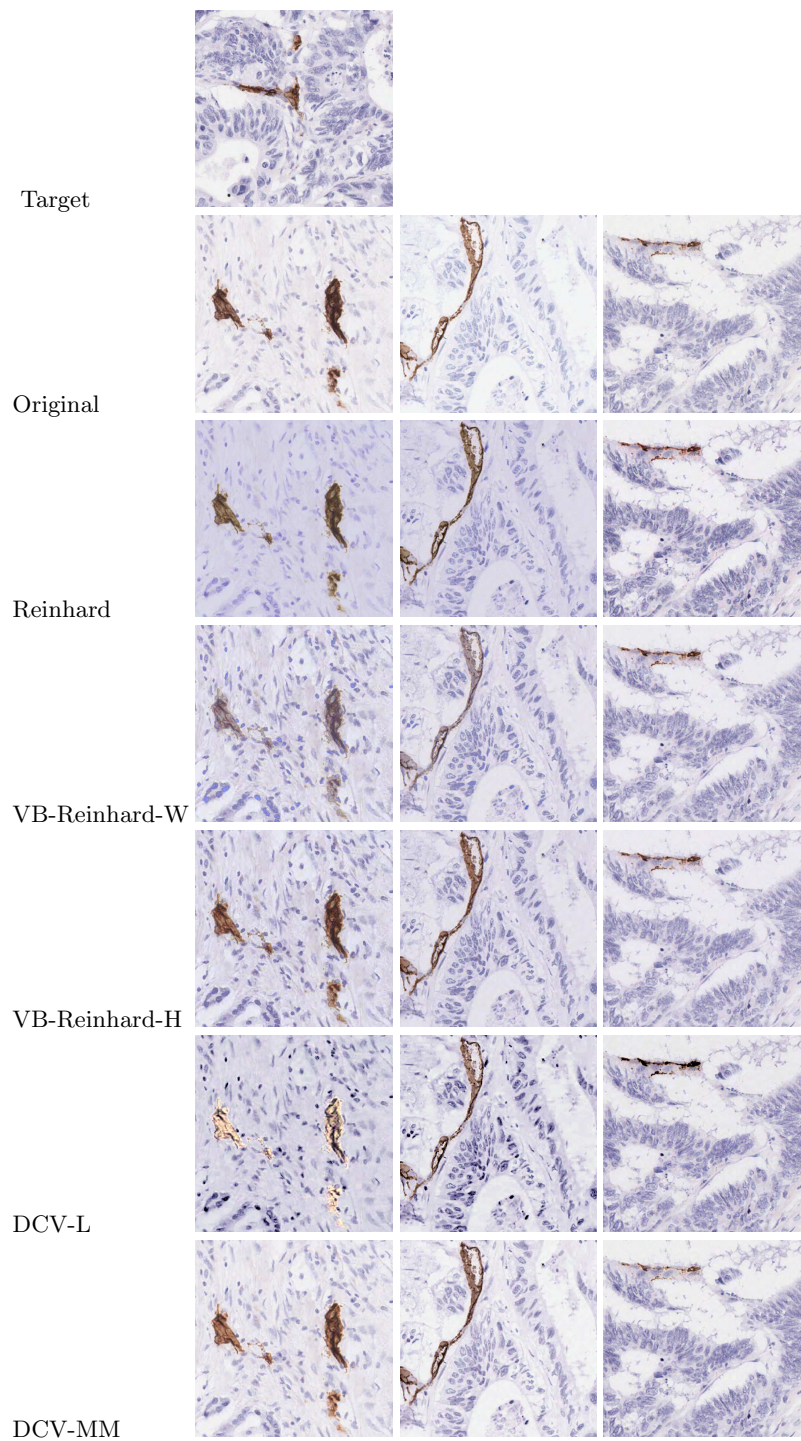


Fig. 5. Results of the different methods applied to 3 images of Haematoxylin and DAB stained liver tissue. The first row contains the target image.

original in the case of the stained areas). Reinhard’s method showed reasonable consistency in the stained areas, but poor consistency in the background (correlating with our qualitative observations of background staining); Figure 2.d shows a worrying overlap between the normalised background means and the original Eosin means. Put simply, the background goes pink in some images making it hard to tell the difference between the Eosin and unstained stained areas. This is due to Eosin dominating the statistics of the linear transform as it covers the largest area. The VB-Reinhard-H fails badly on some images due to segmentation errors. VB-Reinhard-W appears less susceptible to such errors. For the DAB set failure modes were; i) Saturated Nuclei; VB-Reinhard-W (4 images), ii) Un-natural/non-uniform colouring of DAB stained areas; VB-Reinhard-W (1 image), VB-Reinhard-H (1 image), CDV-L (4 images), and iii) significant staining of the background; Reinhard (4 images), CDV-L (2 images). Background staining introduced by the Reinhard method shows minimal overlap with the Haematoxylin (However, this data set was 12 images from a single batch). In the quantitative evaluation the CDV-MM method shown the best consistency between the normalised images and the target over all area types (improved from the original in the case of Haematoxylin stained areas, although initial DAB consistency was reasonable for this data set). All other methods actually decreased the consistency of at least one area type. The second best methods appears to be the VB-Reinhard-H method that failed quite badly on the H&E data. This is likely to be due to the fact that the DAB data does not exhibit the low colour saturation seen in some examples in the H&E set, making the segmentation problem easier. However, at least one image normalised by the VB-Reinhard-H method exhibits artifacts clearly resulting from erroneous segmentation. In conclusion we have demonstrated the inconsistencies in colour in data prepared in the same lab. All methods, except the CDV-MM method, exhibit undesirable failure modes. A useful additional result is that colour deconvolution vectors can often be estimated based on automatic segmentations, even if the segmentation is imperfect. This has scope for application beyond colour normalisation. A summary of the methods evaluated is presented in table 1.

We believe the main problem with the segmentation approach presented in section 2.3 is the unimodal prior for the stain colours used. Different slides can have a wide range of colour values for the same set of stains due to various factors (see section 1) and the distribution of this variation is not well modelled by a unimodal prior. In ongoing work we are working on a Support Vector Machine based method using a Radial Basis Function kernel to perform segmentation. With this approach the multi-modal nature of the data can be modelled. Initial results suggest this gives superior segmentation results to the approach presented in section 2.3, with >95% accuracy (even on images with poor contrast). This is certainly high enough accuracy to calculate colour deconvolution vectors from (and thus perform Colour deconvolution based normalisation). It remains to be seen if this approach is accurate enough not to introduce artifacts when used with the methods in section 2.3. Results of this will be presented at a later date.

References

1. Lyon, H., Leenheer, A.D., et. al.: Standardization of reagents and methods used in cytological and histological practice with emphasis on dyes, stains and chromogenic

Reinhard et al. [6]	If one stain dominates the area this method works well for that stain, but can have an undesirable effect on the other stain (e.g. turning nuclei black) and on the background (turning the background the colour of the dominant stain if that stain is increased in saturation by the transform). If no one stain dominates normalisation performance is poor.
VB Reinhard Hard	This can work well if segmentation performance is good. However, even minor segmentation errors can introduce artifacts in the transformed image.
VB Reinhard Weighted	This is less susceptible to minor segmentation errors than the VB Reinhard Hard method (in terms of introduced artifacts), but if colour distributions of the two stains are close then r_{nk} for a pixel clearly stained by a single stain may not be near 1 for that stain and 0 for the other classes. Therefore, colour matching to the target image can be poor.
DCV Linear	This is a very poor method if areas covered by any stain are small. It is almost always the case that at least one stain stains a minority of pixels, thus the transform for this stain is dominated by background variation/noise, rather than the colour characteristics of the stain.
DCV Multi Modal	This method works the best on the data sets evaluated resulting in no major visible artifacts and good matching with the target images. The main disadvantage is the necessity for image specific colour deconvolution vectors. However, in many cases these may be estimated automatically using automatic image segmentation, or semi-automatically from a simple interactive segmentation.

Table 1. Summary of the Characteristics of Evaluated Methods

- reagents. *Histochemical Journal* **26** (1994) 533–544
2. Finlayson, G., S.Hordey, Hubel, P.: Colour by correlation: A simple, unifying approach to colour constancy. *IEEE Transactions on Pattern Analysis and Machine Intelligence* **23**(11) (2001) 1209–1216
 3. Hamilton, P., Bartels, P., Thompson, D., Anderson, N., Montironi, R.: Automated location of dysplastic fields in colorectal histology using image texture analysis. **182**(1) (1999) 68–75
 4. Qureshi, H., Sertel, O., Rajpoot, N., Wilson, R., Gurcan, M.: Adaptive discriminant wavelet packet transform and local binary patterns for meningioma subtype classification. In: *Proc. Medical Image Computing and Computer-Assisted Intervention*. (2008) 196 – 204
 5. Wang, Y., nd L. Wu, S.C., Tsai, S., Sun, Y.: A color-based approach for automated segmentation in tumor tissue classification. In: *Proc. Conf. of the IEEE Engineering in Medicine and Biology Society*. (2007) 6577–6580
 6. Reinhard, E., Adhikhmin, M., Gooch, B., Shirley, P.: Color transfer between images. *IEEE Computer Graphics and Applications* **21**(5) (2001) 34–41
 7. Ruifrok, A., Johnston, D.: Quantification of histochemical staining by color deconvolution. *Analytical & Quantitative Cytology & Histology* **23** (2001) 291–299
 8. Ruderman, D., Cronin, T., Chiao, C.: Statistics of cone responses to natural images. *Journal of the optical Society of America* **15**(8) (1998) 2036–2045
 9. Bishop, C.: *Pattern Recognition and Machine Learning*. Springer (2006)